Original Article

Monitoring the Progression of Renal Fibrosis by T2-weighted Signal Intensity and Diffusion Weighted Magnetic Resonance Imaging in Cisplatin induced Rat Models

Huan-Huan Wu[1], Hui-Ru Jia[2], Yi Zhang[2], Le Liu[3], Dong-Bo Xu[4], Hao-Ran Sun[1]

[1]Department of Radiology, Tianjin Medical University Hospital, Tianjin, China
[2]Department of Radiology, Northwest Women and Children's Hospital, Tianjin Medical University Hospital, Tianjin, China
[3]Department of Radiology, The Second Affiliated Hospital of Xi'an Jiaotong University, Tianjin Medical University Hospital, Tianjin, China
[4]Department of Pathology, Tianjin Medical University Hospital, Tianjin, China

Abstract

Background: Diffusion weighted imaging (DWI), with the applying of intravoxel incoherent motion model, has showed promising results in obtaining additional information about microperfusion and tubular flow associated with morphologic changes in chronic kidney diseases. The study aims to evaluate the potential of T2-weighted signal intensity (SI) and DWI with mono- and bi-exponential models to reflect the serial changes on cisplatin (CP) induced rat renal fibrosis models.

Methods: Magnetic resonance exams were performed prior to and 2nd day, 4th day, 6th day, 8th day, 2nd week, 3rd week and 4th week after CP injection at a 3.0T with an animal coil. Besides T2-weighted images (T2WI), DWI of 13 *b* values from 0 to 1500 s/mm^2 was acquired. Apparent diffusion coefficient (ADC), fluid fraction *f*, pure diffusivity *D* and pseudodiffusivity *D** values were calculated. The regions of interest were placed on cortex (CO), outer stripe of the outer medulla (OM) and inner stripe of the outer medulla (OM), parameters were measured and compared among different time points. Five rats were scarified at each time point for pathological examination.

Results: OM revealed remarkable hyperintense and broadened before it became an obscure thread, while CO demonstrated moderate hyperintense and IM didn't show significant change on T2WI. On all three stripes, ADC values decreased firstly then kept increasing since the 4th day; *f* values decreased on all stripes; *D* values had a tendency to increase with fluctuations but the changes didn't achieve statistical significance; *D** values increased at the 2nd day then tended to be steady thereafter. Pathological findings revealed tubules epitheliums swelling followed by inflammation cells infiltration, interstitial fibrosis was observed since the 2nd week.

Conclusions: All of T2-weighted SI, ADC, and biexponential models parameters vary during fibrotic process; biexponential model is superior to monoexponential model in separating changes of microperfusion together with tubular flow from pure diffusion.

Key words: Apparent Diffusion Coefficient; Animal Model; Histopathology; Chronic Kidney Disease; Kidney; Renal Fibrosis; Diffusion Weighted Imaging

Introduction

Chronic kidney disease (CKD) is defined as a progressive loss in renal function over a time span of 3 months and longer. Approximately, 6.1 ~ 10% of the general population in China have CKD, with an even higher risk in people older than 40 years. CKD may be caused by a wide spectrum of diseases.[1] The common pathological consequences of CKD is renal fibrosis, assessment of the continuous deterioration of renal fibrosis is important.[2] Renal biopsy is unsurprisingly the golden standard to determine the degree of renal fibrosis in patients; however, it is an invasive method and inconformity for repeatedly monitoring the progression of fibrosis in clinical follow-up, and it remains challenging to establish a noninvasive biomarker to monitor the progression or regression of renal fibrosis in substitute of biopsy.

Magnetic resonance imaging (MRI) could provide both high spatial resolution and excellent tissue contrast in evaluating morphologic alteration in CKD. Moreover, diffusion weighted imaging (DWI) MRI has showed more promising results in assessing renal function.[3] The commonly used quantitative parameter to interpret DWI is apparent diffusion coefficient (ADC) value. ADC is calculated by fitting the signal intensities (SIs) from a series of DWI with different diffusion weightings (*b* values) using a monoexponential model. Previous reports revealed that the CKD patients have

Access this article online

Quick Response Code:

Website: www.cmj.org

DOI: 10.4103/0366-6999.151660

Address for correspondence: Dr. Hao-Ran Sun, Department of Radiology, Tianjin Medical University Hospital, Tianjin 300052, China
E-Mail: sunhaoran2006@hotmail.com

significantly lower ADC values in the cortex and medulla,[4] and found that ADC was able to assess the degree of renal fibrosis in unilateral ureteral obstruction murine models.[5]

In 1986, Le Bihan *et al*. introduced the principles of intravoxel incoherent motion (IVIM).[6] The concept leads to a more dedicated approach to enable tissue diffusivity and microperfusion to be quantitatively estimated separately. It could be speculated that additional information about microperfusion and tubular flow obtained with IVIM DWI may be especially helpful to evaluate the progress of renal fibrosis.[7]

The study aims to evaluate the potential of T2-weighted SI and DWI with mono-and bi-exponential models to reflect the serial changes of both morphology and function on cisplatin (CP) induced rodent renal fibrosis models with reference to the corresponding pathological observations.

Methods

Animal model

This study was approved by Animal Care and Use Committee, Tianjin Medical University Hospital. A total of 45 male Sprague-Dawley rats (Beijing University Health Science Center) weighted 226 ± 25 g were used. Renal fibrosis was induced by intraperitoneal injection of CP solution (QILU Pharmaceutical Company Shandong, China, Batch Number:WA2A1210071) 4.5 mg kg^{-1} day^{-1} in 2 consecutive days. After injection, rats were marked and raised in clean plastic cages in a temperature- and humidity-controlled facility with a constant 12 h light/dark cycle. All rats showed intoxication symptoms including fatigued, loss of appetite, diarrhea, and weight losing especially during the 1st week after CP injection. Nine rats died from serious diarrhea (n = 6) or anesthetic accident (n = 3), finally 36 rats enrolled in the present study. The rats were randomly selected to undergo MR scanning immediately before (n = 21) and 2 days (n = 24), 4 days (n = 24), 6 days (n = 23), 8 days (n = 18), 2 weeks (n = 11), 3 weeks (n = 8) and 4 weeks (n = 6) after CP injection.

Magnetic resonance imaging protocol

MR examination was performed on a 3.0T scanner (MR750, GE Company, US) using an 5 cm inner diameter animal coil (Magtron, China) under a stable anesthetized condition by intramuscular injection of 2% pentobarbital sodium solution (0.15 ml/100 g weight). Rats were fasting but free of drinking 2 h before MR exam and respiratory movement was restricted by proper compression on the abdominal region. Coronal fat suppressed fast recovery fast spin echo T2-weighted images were acquired with following parameters: Repetition time/echo time (TR/TE) 3182.6 ms/94.1 ms, matrix 352 × 352, field of view 6.0 cm, thickness 2.0 mm, spacing 0.5 mm, bandwidth ± 83.3 kHz, two signal averaged with a total acquisition time of 4 min 44 s. Axial multisection single shot-echo planar imaging (EPI) DWI was acquired with the following parameters: TR/TE 2075/111.9 ms; 10 sections coving both kidney regions, section thickness 2 mm, intersection spacing 0.5 mm, field of view 6.0 cm, matrix 192 × 96, bandwidth ± 100 kHz. The following 13 diffusion gradient b values were used: 0, 20, 40, 60, 80, 100, 140, 180, 240, 300, 500, 1000 and 1500 s/mm^2, the gradients were applied in three orthogonal directions and subsequently averaged to minimize the effects of diffusion anisotropy. The numbers of signal average gradually rose from 2 to 8 along with the increasing b value; the acquisition time was 2 min 45 s.

Image analysis

The MRI data series was transferred to an offline workstation (ADW4.5, GE Company, US). Both morphologic changes and functional changes were evaluated on the workstation singly by two radiologists with 15-year and 3-year experience in urogenital imaging respectively.

The morphologic changes of the renal parenchyma were evaluated on coronal T2WI. Besides visual inspection, the regions of interest (ROI) were placed free-hand on entire regions of renal cortex (CO), the outer stripe of the outer medulla (OM) and the inner stripe of the inner medulla (IM) at the middle coronal section of bilateral kidneys and average SI were measured. To reflect the signal changes on T2WI, T2-weighted standardized SIs were obtained by calculating the ratios between the average SIs of each of the three stripes and SI of homolateral psoas major.

Functional data of DWI were analyzed using Microsoft Data Access Components (MADC) software in the functiontools package installed in the workstation. Both monoexponential model (equation 1) and biexponential model (equation 2) were used on the same multiple b value DWI data series.[8]

$$S(b)/S(0) = \exp(-b \times ADC) \quad (1)$$

$$S(b)/S(0) = (1-f)\cdot e^{-bD} + f\cdot e^{-b\cdot(D^*+D)} \quad (2)$$

S (0) is the SI in DWI for $b = 0$ (b_0). S (b) is the SI in a serial of DWI acquired by different b values. ADC maps were generated on renal parenchyma pixel-by-pixel by fitting the SIs with corresponding b values to a monoexponential decay model. Biexponential model yielded three parameters: f refers to the ratio of flow content in the entire volume, it reflects tissue microvasculature as well as tubular flow; D reflects pure diffusion coefficient and is sensitive to microstructural barriers, which limit slow water molecular movement; D^* indicates pseudodiffusivity of fast water molecular movement which is sensitive to flow velocity.

After ADC, f, D and D^* maps were generated, ROIs of entire CO, OM and IM stripes were plotted on the renal helium section according on the b = 0 images and transferred to the maps. The average value of ADC, f, D and D^* of the three stripes were measured on bilateral kidneys respectively.

Histopathological examination

Five rats were randomly scarified after MRI examination

accomplished at each time point after CP administration. Both kidneys were harvested for histopathological examination. The specimens were fixed in 5% buffered formalin and processed, then cut serially into 5 mm thickness section, and stained with hematoxylin and eosin pathological findings including tubules swelling and necrosis, inflammation cells infiltration in tubulointerstitium and the progression of renal fibrosis was assessed visually by an experienced pathologist.

Statistical analysis

Results are presented as mean ± standard deviation. The measurements of bilateral kidneys in each subject were analyzed for discrepancies by paired student *t*-test. The Intraclass correlation coefficient (ICC) was calculated to evaluate the reliability between the observers and the average values. The measured parameters on bilateral kidneys by the two observers were then averaged. The data were analyzed by the way of independent sample *t*-test among different time points. The discrepancies among each time point were statically analyzed on CO, OM and IM stripes respectively. For all statistical tests, a $P < 0.05$ was considered to be statistically significant. Statistical analyses were performed with Statistical Product and Service Solutions(SPSS) software 12.0.1 and Microsoft Office Excel 2003 workbook (Microsoft Company).

Results

There was no significant difference in all the measurement between bilateral kidneys on all the three stripes ($n = 675$, $P = 0.94$). Interobserver agreement ICCs were ranged from 0.66 to 0.99 for OM, 0.73–0.99 for CO and 0.76–0.98 for IM.

Morphologic evaluation on magnetic resonance imaging

Observation of standardized signal intensity on renal fibrosis rats

Cortex (2.35 ± 0.40) and OM (2.35 ± 0.40) couldn't be distinguished between each other, and IM showed relative hyperintense (3.13 ± 0.61) prior to CP injection. Two days after CP injection, OM began to appear as a hyperintense stripe (3.78 ± 0.72, $P < 0.05$) with distinct boundaries with CO and IM; then it gradually broadened and became less intense with transit downward fluctuation but beyond normal level during 4th day and 4th week ($P < 0.05$), consequently it shrink to be an obscure thread 4 weeks after CP injection. CO revealed slightly increased intensity (2.60 ± 0.41, $P < 0.05$) at the 2nd days after injection, then decreased to normal level (2.28 ± 0.51, $P > 0.05$) 2 days later then appeared as steady hyperintense thereafter ($P < 0.05$). IM showed the transit and moderate hypointense (2.52 ± 0.72, $P < 0.05$) at only 4th day [Figures 1 and 2].

Functional evaluation on magnetic resonance imaging

Observation of apparent diffusion coefficient values on renal fibrosis rats

Mean ADC values of all the CO, OM and IM decreased firstly and then kept increasing since the 4th day. The mean ADC values of OM were higher than normal subject ($4.38 \pm 0.63 \times 10^{-4}$ mm^2/s vs. $4.91 \pm 0.56 \times 10^{-4}$ mm^2/s, $P < 0.05$), while the ADC values of CO were similar to normal level ($5.7 \pm 0.79 \times 10^{-4}$ mm^2/s, $P > 0.05$) since the 6th day. The changes of ADC values for OM and CO tended to be stable during the 6th and 4th week ($P > 0.05$). In IM, excepted for the 4th week ($4.33 \pm 0.93 \times 10^{-4}$ mm^2/s, $P = 0.07$), mean ADC values were significant lower than normal subjects ($5.23 \pm 1.05 \times 10^{-4}$ mm^2/s) at all time points ($P < 0.05$) [Figure 3a].

Observation of bi-exponential models on renal fibrosis rats

The *f* values of all the CO, OM and IM stripes decreased after CP injection and were below normal level all the time ($P < 0.05$), and the changes in OM were more remarkable [Figure 3b]. The slow recovery of *f* values were seen as early as 4th day in IM, then 6th in CO, but *f* values in OM kept decreasing till 8th day before going steadily upward ($P < 0.05$).

D values of CO, OM and IM stripes, on the contrary to *f* values, had a tendency to increase in spite of some downward fluctuations [Figure 3c]; however, changes on CO and OM were not significant at all time points when compared with healthy kidneys (CO: mean $0.31 \pm 0.28 \times 10^{-3}$ mm^2/s; OM: $1.04 \pm 0.80 \times 10^{-3}$ mm^2/s) ($P > 0.05$). *D* values of IM kept increasing till the 2nd week as in Figure 3c, then turned back to normal level; however, the difference between each time point and healthy kidney ($1.12 \pm 1.51 \times 10^{-3}$ mm^2/s) wasn't significant ($P > 0.05$), resulting from the standard deviations of *D* values on IM were large at all the time points.

*D** values of CO, OM and IM stripes has a similar upward trend at the 2nd day, and then tended to be steady thereafter till the 3rd week [Figure 3d]. At all the time points except for 4th week, *D** values of three stripes were significant higher than healthy kidneys ($P < 0.05$). Mean *D** values of IM ($7.33 \pm 3.99 \times 10^{-2}$ mm^2/s) were higher than CO ($2.50 \pm 2.13 \times 10^{-2}$ mm^2/s and OM ($3.77 \pm 2.47 \times 10^{-2}$ mm^2/s) in healthy kidneys ($P < 0.05$).

Serial histopathology findings on renal fibrosis rats

At the 2nd and 4th day after CP injection, the epitheliums of renal tubules showed obviously cell swelling and tubules narrowing, and OM stripes which was consisting of proximal convoluted tubules demonstrated the most remarkable changes [refer to the acute stage, Figure 4a]. During the 6th and 8th day, cell swelling relieved while cell turbidity and renal tubular mold could be observed, massive inflammation cells began to infiltrate in the interstitium [refer to the chronic stage, Figure 4b and c]. Renal interstitial fibrosis was initially observed at 2nd week; tubular atrophy and necrosis, broadened interstitial space with proliferation of myofibroblasts and cellular density increasing could be demonstrated throughout the fibrotic process after the 3rd week [refer to the fibrosis stage, Figure 4d].

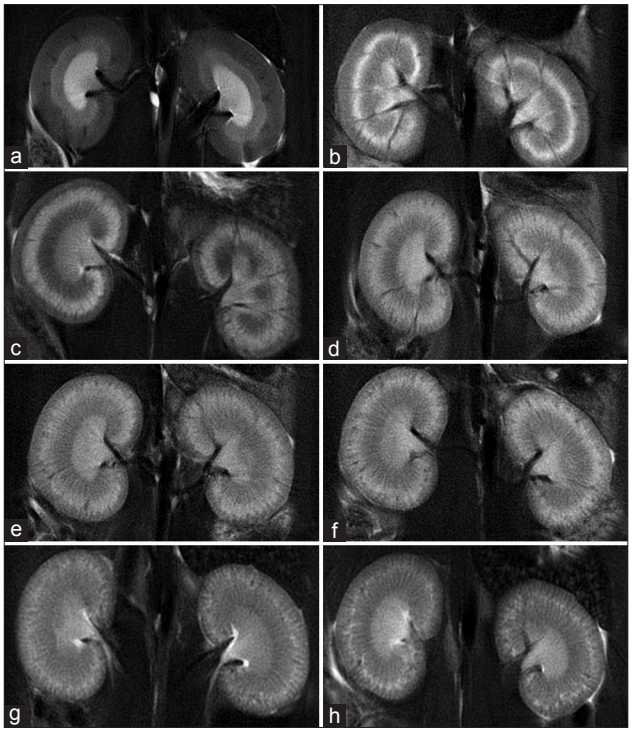

Figure 1: Serial morphologic changes of rat bilateral kidneys prior to and after CP injection on coronal fat suppressed fast recovery fast spin echo T2-weighted images. (a) Healthy kidneys; (b-h) 2nd day, 4th day, 6th day, 8th day, 2nd week 3rd and 4th week after CP injection. On healthy kidneys prior to CP injection, CO and OM showed similar moderate signal intensity, and IM showed relative hyperintense. After CP injection, OM revealed a remarkable hyperintense stripe with distinct boundaries with CO and IM; it gradually broadened and became obscure and less hyperintense till the 4th week after CP injection. CO revealed slightly increased intensity at the 2nd days, then decreased to the normal level 2 days later and kept increasing thereafter. IM changed slightly during the process. CP: Cisplatin; OM: Outer stripe of outer medulla; IM: Inner stripe of outer medulla; CO: Renal cortex.

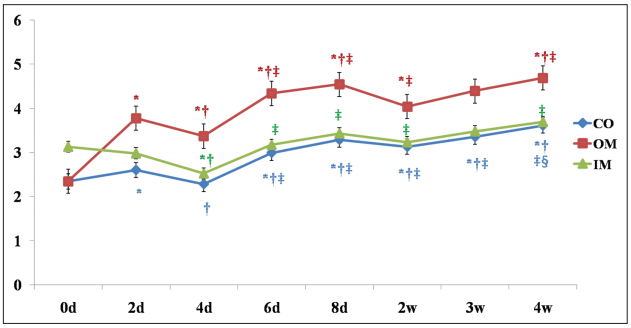

Figure 2: Serial changes of SSI on three stripes of the renal parenchyma in rats prior to and at different time points after CP administration. CO: Renal cortex; CP: Cisplatin; SSI: Standardized signal intensity; OM: Outer stripe of the outer medulla; IM: Inner stripe of the outer medulla. SSI of OM was higher than the other two. $^{*}P < 0.05$ compared with normal kidney; $^{\dagger}P < 0.05$ compared with the 2nd day after kidney CP administration; $^{\ddagger}P < 0.05$ compared with the 4th day after kidney CP administration; $^{\S}P < 0.05$ compared with the 6th day after kidney CP administration; $^{||}P < 0.05$ compared with the 8th day after kidney CP administration; $^{\P}P < 0.05$ compared with the 2nd week after kidney CP administration; $^{**}P < 0.05$ compared with the 3nd week after kidney CP administration.

Discussion

From the findings of this longitudinal study, all of T2-weighted SI, ADC value, and biexponential parameters showed variations that agree with pathologic observations. Unlike human and swine kidneys, which are multilubular in anatomic structure, rodent kidneys are unilobular, this is ideal to delineating among different anatomic regions. Rodent kidney parenchyma is divided into four stripes: CO contains all glomeruli and their corresponding proximal convoluted tubules, OM is mainly occupied by the tortuous proximal convoluted tubules, IM is consisting of descending thin limbs and thick ascending limbs, and the inner medulla stripe is occupied by renal collecting ducts.[9] Rodent renal fibrosis models have been successfully induced by administration of CP in a large number of histopathologic studies. CP is a widely used antineoplastic agent, but associated with nephrotoxicity, and prone to result in long-term renal fibrosis after administration, the damages involve both glomeruli and tubules, while the major damage happens in proximal convoluted tubules.[10] The pathologic changes of inner medulla in CKD is minor, true but without shown in the present study, the inner medulla is isointense to renal pelvis which makes it difficult to be delineated; hence the analysis of inner medulla is neglected in the study.

The standardized T2-weighted SIs that are sensitive to tissue edema and necrosis were introduced in this study to evaluate morphological changes of renal fibrosis. The elevated T2-weighted SI, predominately seen on OM in the early stage implied the happening of acute cytotoxic edema and tubular necrosis that was proved histopathologically. However, T2-weighted SIs were then going in a steady state that was inconsistent with fibrotic progression. Similar observation was described by Hueper *et al*. on acute kidney injury mice,[11] suggesting T2-weighted SI could not stand alone by itself to be a biomarker of renal fibrosis.

Several investigators have reported decreased ADC in both cortex and medulla in CKD patients or renal fibrosis animal model compared with normal subjects.[5,12,13] The ADC values of cortex and medulla after CP administration were initially decreased as expected, however, both CO and OM had a tendency to increase and were higher than that of normal kidney since 6 days after CP injection, at times inflammation and fibrosis were observed. This phenomenon is controversial with most of the published data; the elevation of ADC values in diseased tissues was described in few reports with increased microperfusion.[14] The ADC values behaved as a weight of the pure diffusion and pseudodiffusion, pure diffusion restriction was mainly depending on the cellularity which was increasing during fibrogenic process,[5] hence the increasing of pseudodiffusion should be responsible for the ADC upward alteration.

Intravoxel incoherent motion is capable of separating pure diffusion and microperfusion theoretically, which is beneficial beyond simple ADC in oncology imaging and

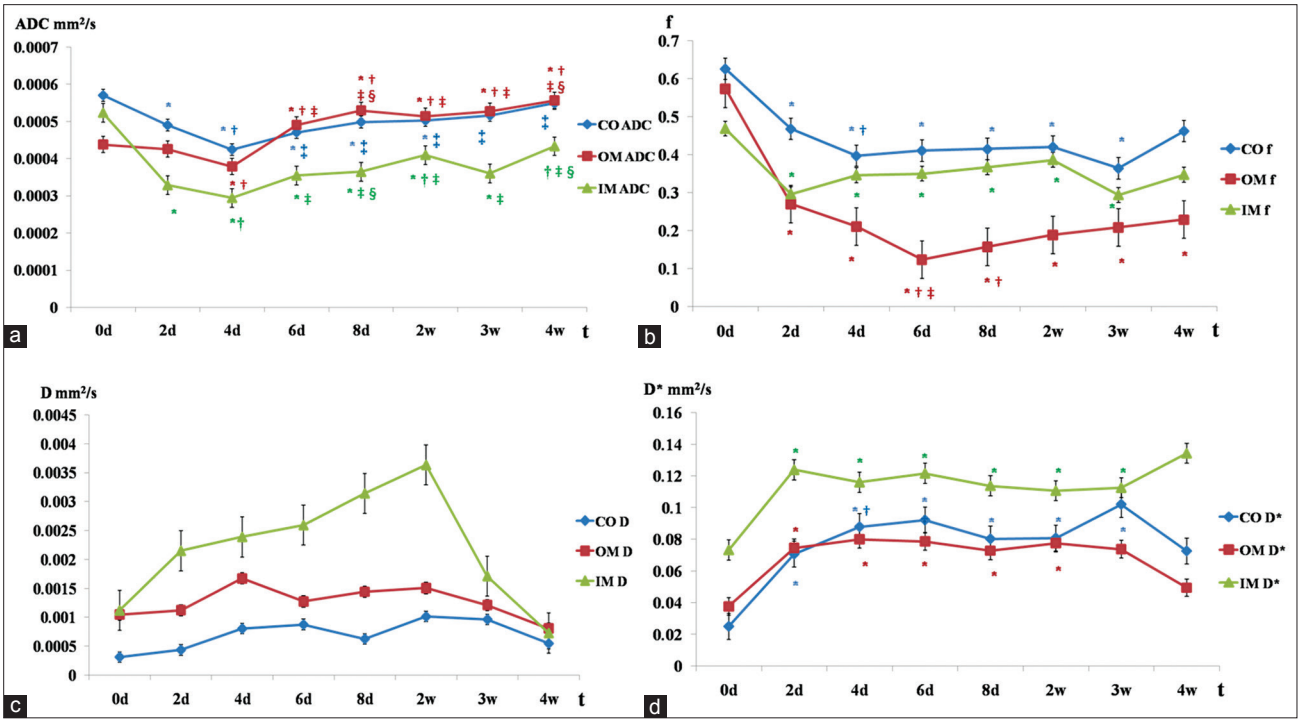

Figure 3: Serial changes of mono-exponential and biexponential models parameters on renal parenchyma in rats prior to and at different time points after CP administration. (a) Serial changes of ADC value. ADC values decreased firstly then kept increasing since the 4th day; (b) Serial changes of *f* fractions. The *f* values of all three stripes were below the normal level after CP injection, and the changes on OM were more remarkable; (c) Serial changes of *D* values. *D* values had a tendency to increase with downward fluctuation; (d) Serial changes of *D** values. *D** values of CO, OM and IM stripes increased at the 2nd day, and then tended to be steady thereafter till the 3rd week. CO: Renal cortex; CP: Cisplatin; ADC: Apparent diffusion coefficient; OM: Outer stripe of the outer medulla; IM: Inner stripe of the outer medulla. $^{*}P < 0.05$ compared with normal kidney; $^{\dagger}P < 0.05$ compared with the 2nd day after kidney CP administration; $^{\ddagger}P < 0.05$ compared with the 4th day after kidney CP administration; $^{\S}P < 0.05$ compared with the 6th day after kidney CP administration; $^{||}P < 0.05$ compared with the 8th day after kidney CP administration; $^{\P}P < 0.05$ compared with the 2nd week after kidney CP administration; $^{**}P < 0.05$ compared with the 3nd week after kidney CP administration.

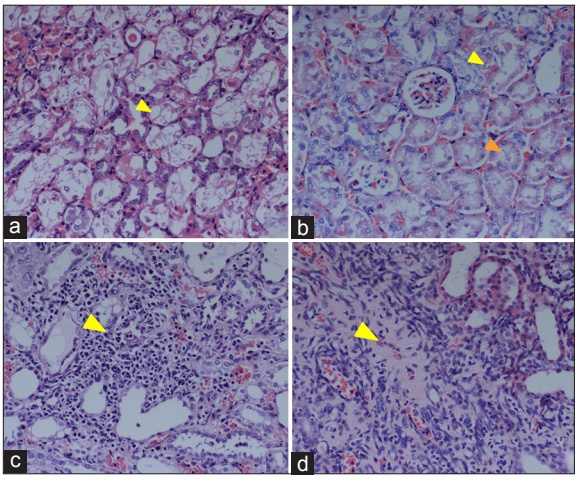

Figure 4: Serial pathological changes of the renal parenchyma in rats after CP administration (H and E, ×200). (a) At the 2nd day after CP injection, the epitheliums of renal tubules showed obviously cell swelling; (b) At the 6th day, cell turbidity (yellow arrow) and renal tubular mold could be observed (orange arrow); (c) At the 8th day, inflammation cells infiltrated in renal interstitium (arrow) resulting in cellularity increasing; (d) At the 4th week, massive fibrotic collagen (arrow) within broadened renal interstitial space was demonstrated together with tubular atrophy. CP: Cisplatin.

functional imaging. The model hypothesizes that the tissue signal decay *in vivo* might be divided into flow-dependent fast decay and flow independent slow decay, which makes it particularly meaningful in evaluating renal diseases.[15] The water movement within extracellular space is modeled as pure diffusivity when DWI are acquired with higher *b* value (over 600–800 s/mm^2), while the microapillary perfusion and tubular flow are classified as pseudodiffusion, which is predominant with low *b* values (under 100–200 s/mm^2). Recent studies demonstrated the capability of IVIM in differencing subtypes of renal tumors.[16] Zhang *et al*. showed that the biexponential parameters were more accurate than monoexponential ADC in healthy volunteers.[4]

Among of three parameters in biexponential model, *f* fraction of all stripes showed early decreasing and subsequent recovering process. *F* fraction referred to the proportion of fast flow contents in overall diffusion effect. Therefore, the decrease of *f* value indicated both the lessened capillary vasculature and narrowed renal tubular which is coincident with pathology. Meanwhile, the *D* values of CO, OM and IM had a tendency to increase after CP injection but failed to demonstrate significant alterations during the period of observation. The steady state of *D* values were also observed in some but disagree with the majority of published data, and it agreed with our previous study on unilateral ureteral obstruction rat model, which

demonstrating increased *D* value along with time.[17] Pure diffusivity was also affected by a number of imaging factors including signal to noise ratios, registration artifacts, field strength, imaging sequence, and parameters, as well as the *b* value setting.[4,18] However, it wouldn't interfere with a longitudinal study design like ours, the reason of *D* value increasing instead of decreasing during renal fibrosis was unclear and under investigation. *D** values of all stripes increased after CP injection, and the mean *D** values of IM were higher than the others. The pseudodiffusion *D** of the renal parenchyma depends on both microperfusion and tubular flow, the elevated *D** value suggested either increased microcirculation or faster renal tubular flow. Ebrahimi *et al*. suggested that *D** mainly depended on the velocity of tubular fluid instead of microperfusion in the kidney by correlated IVIM parameters with computed tomography perfusion parameters on swine model.[19] According to the pathological observation, with the progressing of renal fibrosis, destroy, and atrophy of renal tubular was common seen, then tubular flow velocities would increase as compensating and repairing mechanisms, which were intermingled together. A higher *D** in IM implied that there existed faster tubular fluid flow in descending and ascending limbs than proximal convoluted tubules, which was rational on the basis of renal physiology.

The study had some limitations. Because of intrinsic distortion of EPI, separately analysis of the stripes prone to error because of small ROI size; large variations might have prevented the achievement of statistical significance. The ridicules that makeup of proximal convoluted tubules extends from OM to CO had blurred the boundary between them, hence the arbitrarily ROI delineating between OM And CO leading the large variations of parameters. A more robust Gaussian distribution model and auto segmentation techniques might be helpful in further investigation. Although the present data rendering the feasibility that the microperfusion together with tubular dynamics might be evaluated using biexponential models, they couldn't be separated from each other by IVIM method. Finally, the study is lack of evidence of specific pathologic finding for renal fibrosis such as cellularity counting and assessment of microperfusion and tubular dynamics alterations, a correlation study with IVIM parameters would be more convincing in future study.

References

1. Wang F, Zhang L, Wang H, China National Survey of CKD Working Group. Awareness of CKD in China: A national cross-sectional survey. Am J Kidney Dis 2014;63:1068-70.
2. Drawz PE, Rosenberg ME. Slowing progression of chronic kidney disease. Kidney Int Suppl (2011) 2013;3:372-76.
3. Müller MF, Prasad PV, Bimmler D, Kaiser A, Edelman RR. Functional imaging of the kidney by means of measurement of the apparent diffusion coefficient. Radiology 1994;193:711-5.
4. Zhang JL, Sigmund EE, Chandarana H, Rusinek H, Chen Q, Vivier PH, *et al.* Variability of renal apparent diffusion coefficients: Limitations of the monoexponential model for diffusion quantification. Radiology 2010;254:783-92.
5. Togao O, Doi S, Kuro-o M, Masaki T, Yorioka N, Takahashi M. Assessment of renal fibrosis with diffusion-weighted MR imaging: Study with murine model of unilateral ureteral obstruction. Radiology 2010;255:772-80.
6. Le Bihan D, Breton E, Lallemand D, Grenier P, Cabanis E, Laval-Jeantet M. MR imaging of intravoxel incoherent motions: Application to diffusion and perfusion in neurologic disorders. Radiology 1986;161:401-7.
7. Krier JD, Ritman EL, Bajzer Z, Romero JC, Lerman A, Lerman LO. Noninvasive measurement of concurrent single-kidney perfusion, glomerular filtration, and tubular function. Am J Physiol Renal Physiol 2001;281:F630-8.
8. Le Bihan D, Breton E, Lallemand D, Aubin ML, Vignaud J, Laval-Jeantet M. Separation of diffusion and perfusion in intravoxel incoherent motion MR imaging. Radiology 1988;168:497-505.
9. Christensen EI, Grann B, Kristoffersen IB, Skriver E, Thomsen JS, Andreasen A. Three-dimensional reconstruction of the rat nephron. Am J Physiol Renal Physiol 2014;306:F664-71.
10. Lieberthal W, Triaca V, Levine J. Mechanisms of death induced by cisplatin in proximal tubular epithelial cells: Apoptosis vs. necrosis. Am J Physiol 1996;270:F700-8.
11. Hueper K, Rong S, Gutberlet M, Hartung D, Mengel M, Lu X, *et al.* T2 relaxation time and apparent diffusion coefficient for noninvasive assessment of renal pathology after acute kidney injury in mice: Comparison with histopathology. Invest Radiol 2013;48:834-42.
12. Rheinheimer S, Schneider F, Stieltjes B, Morath C, Zeier M, Kauczor HU, *et al.* IVIM-DWI of transplanted kidneys: Reduced diffusion and perfusion dependent on cold ischemia time. Eur J Radiol 2012;81:e951-6.
13. Heusch P, Wittsack HJ, Pentang G, Buchbender C, Miese F, Schek J, *et al.* Biexponential analysis of diffusion-weighted imaging: Comparison of three different calculation methods in transplanted kidneys. Acta Radiol 2013;54:1210-7.
14. Sigmund EE, Vivier PH, Sui D, Lamparello NA, Tantillo K, Mikheev A, *et al.* Intravoxel incoherent motion and diffusion-tensor imaging in renal tissue under hydration and furosemide flow challenges. Radiology 2012;263:758-69.
15. Lee CH, Yoo KH, Je BK, Kim IS, Kiefer B, Park YS, *et al.* Using intravoxel incoherent motion MR imaging to evaluate cortical defects in the first episode of upper urinary tract infections: Preliminary results. J Magn Reson Imaging 2014;40:545-51.
16. Chandarana H, Lee VS, Hecht E, Taouli B, Sigmund EE. Comparison of biexponential and monoexponential model of diffusion weighted imaging in evaluation of renal lesions: Preliminary experience. Invest Radiol 2011;46:285-91.
17. Jia HR, Zhang Y, Liu L, Wu HH, Han W, Gao W, *et al*. Assessment of renal changes in diffusion and microperfision with mono-and bi-exponential models DW MRI on unilateral ureteral obstruction rats. Chin J Med Imaging 2014;22:326-9.
18. Rheinheimer S, Stieltjes B, Schneider F, Simon D, Pahernik S, Kauczor HU, *et al.* Investigation of renal lesions by diffusion-weighted magnetic resonance imaging applying intravoxel incoherent motion-derived parameters – Initial experience. Eur J Radiol 2012;81:e310-6.
19. Ebrahimi B, Rihal N, Woollard JR, Krier JD, Eirin A, Lerman LO. Assessment of renal artery stenosis using intravoxel incoherent motion diffusion-weighted magnetic resonance imaging analysis. Invest Radiol 2014;49:640-6.

Received: 21-10-2014 **Edited by:** De Wang

How to cite this article: Wu HH, Jia HR, Zhang Y, Liu L, Xu DB, Sun HR. Monitoring the Progression of Renal Fibrosis by T2-weighted Signal Intensity and Diffusion Weighted Magnetic Resonance Imaging in Cisplatin induced Rat Models. Chin Med J 2015;128:626-31.

Source of Support: This work was supported by grant from Chinese Nature Science Foundation (No. 81171316). **Conflict of Interest:** None declared.